Atmos. Chem. Phys. Discuss., https://doi.org/10.5194/acp-2017-463
Manuscript under review for journal Atmos. Chem. Phys.
Discussion started: 12 July 2017

Tropospheric ozone and its precursors at Summit, Greenland: comparison between observations and model simulations

Yaoxian Huang[1,a], Shiliang Wu[1,2,3], Louisa J. Kramer[1,2,b], Detlev Helmig[4], and Richard E. Honrath[1,2,†]

[1]Department of Geological and Mining Engineering and Sciences, Michigan Technological University, Houghton, Michigan, USA

[2]Atmospheric Sciences Program, Michigan Technological University, Houghton, Michigan, USA

[3]Department of Civil and Environmental Engineering, Michigan Technological University, Houghton, Michigan, USA

[4]Institute of Arctic and Alpine Research, University of Colorado, Boulder, Colorado, USA

[a]now at: School of Forestry and Environmental Studies, Yale University, New Haven, Connecticut, USA

[b]now at: University of Birmingham, Birmingham, UK

[†]deceased

Correspondence to: S. Wu (slwu@mtu.edu) and Y. Huang (yaoxian.huang@yale.edu)

Abstract. Recent studies have shown some significant challenges for atmospheric models to simulate tropospheric ozone (O_3) and some of its precursors in the Arctic. In this study, ground based data are combined with a global 3-D chemical transport model (GEOS-Chem) to examine the abundance and seasonal variations of O_3 and its precursors at Summit, Greenland (72.34˚ N, 38.29˚ W, 3212 m.a.s.l). Model simulations for atmospheric nitrogen oxides (NO_x), peroxyacetyl nitrate (PAN), ethane (C_2H_6), propane (C_3H_8), carbon monoxide (CO), and O_3 for the period of 07/2008-06/2010 are compared with observations. The model performs well in simulating certain species (such as CO and C_3H_8), but some significant discrepancies are identified for other species and further investigated. The model generally underestimates NO_x and PAN (by around 50% and 30%, respectively) for March-June. Likely contributing factors to the low bias include missing NO_x and PAN emissions from snowpack chemistry in the model. At the same time, the model overestimates NO_x mixing ratios by more than a factor of 2 in wintertime, with episodic NO_x mixing ratios up to 15 times higher than the typical NO_x levels at Summit. Further

investigation shows that these simulated episodic NO_x spikes are always associated with transport events from Europe, but the exact cause remains unclear. The model systematically overestimates C_2H_6 mixing ratios by approximately 20% relative to observations. This discrepancy can be resolved by decreasing anthropogenic C_2H_6 emissions over Asia and the US by ~ 20%, from 5.4 to 4.4 Tg/yr. GEOS-Chem is able to reproduce the seasonal variability of O_3 and its spring maximum. However, compared with observations, it underestimates surface O_3 by approximately 13% (6.5 ppbv) from April to July. This low bias appears to be driven by several factors including missing snowpack emissions for NO_x and nitrous acid, the coarse model resolution, model overestimated O_3 dry deposition velocity during springtime, as well as the uncertainties in the stratosphere-to-troposphere exchange scheme for O_3.

1. Introduction

Ozone (O_3) and its precursors (e.g., NO_x = NO + NO_2 and volatile organic compounds) are important atmospheric species affecting both air quality and climate (e.g., Jacob et al., 1992; Fiore et al., 2002; Unger et al., 2006). Tropospheric O_3 is a potent greenhouse gas and it also has detrimental effects on human health and vegetation (Knowlton et al., 2004; Hollaway et al., 2012; Yue and Unger, 2014). NO_x is an important precursor for O_3 production and peroxyacetyl nitrate (PAN), which serves as a reservoir for NO_x. PAN, O_3, as well as some of their precursors, have relatively long lifetimes in the atmosphere, enabling them to be transported long distance to remote regions such as the Arctic.

Recent studies have shown some significant challenges for atmospheric chemical transport models to simulate O_3 and its precursors in the Arctic (e.g., Shindell et al., 2008; Alvarado et al., 2010; Walker et al., 2012; Wespes et al., 2012; Fischer et al., 2014; Monks et al., 2015). In the multi-model assessment by Shindell et al. (2008), more than a dozen models all showed systematic and persistent underestimation of O_3 at the GEOSummit station, Greenland (hereafter referred to as Summit). Alvarado et al. (2010) used NO_x and PAN measurements from ARCTAS (Arctic Research of the Composition of the Troposphere from Aircraft and Satellites) in the summer to compare with model simulations. They found that model simulated NO_x mixing ratios were higher than observations, while PAN mixing ratios were lower in fresh boreal fire plumes. In terms of global PAN simulations, Fischer et al. (2014) directly partitioned 40% of NO_x emissions from wildfires to PAN formation, which improved the agreement between model and

observations. However, the model still underestimated PAN surface mixing ratios during springtime in the Arctic. Walker et al. (2012) reported that model simulated O_3 mixing ratios were biased low when compared with balloon data during summertime from two high-latitude sites at Eureka (80˚N, 86˚W) and Ny-Ålesund (79˚, 12˚E). Wespes et al. (2012) also revealed that model simulated O_3 mixing ratios below the boundary layer in the Arctic are significantly underestimated during spring-summer, compared with ARCTAS measurements. More recently, Monks et al. (2015) further demonstrated that model simulated O_3 mixing ratios in the Arctic at the surface and in the upper troposphere were generally lower than the observations.

Global anthropogenic ethane (C_2H_6) emission estimates range from 5.7 Tg/yr to 16.2 Tg/yr (Blake and Rowland, 1986; Kanakidou et al., 1991; Rudolph, 1995; Gutpa et al., 1998; Xiao et al., 2008; Etiope and Ciccioli, 2009; Pozzer et al., 2010; Aydin et al., 2011; Simpson et al., 2012; Emmons et al., 2015; Franco et al., 2016; Tzompa-Sosa et al., 2017), with a decreasing trend from 1980 to 2009 (Simpson et al., 2012; Helmig et al., 2014a). However, since 2009, global anthropogenic C_2H_6 emissions began to increase (Franco et al., 2015; Hausmann et al., 2016; Helmig et al., 2016). The RETRO (REanalysis of the TROpospheric chemical composition) global emission inventory used to be the global default anthropogenic C_2H_6 emission inventory, the annual budget of which has been shown too low compared with observations (Xiao et al., 2008; Fischer et al., 2014; Franco et al., 2015, 2016), whereas the emission inventory from Xiao et al. (2008) has been demonstrated to match observations during 1988-2004. Model simulated C_2H_6 mixing ratios are particularly biased low in the remote high latitude regions, when compared with observations (Emmons et al., 2015).

Field measurements at Summit show that snowpack emits gas-phase NO_x, PAN, nitrous acid (HONO), as well as hydrogen peroxide (H_2O_2) during spring-summer, when polar sun rises (Ford et al., 2002; Honrath et al., 2002). Although several 1-D models (Thomas et al., 2011, 2012; Frey et al., 2013; Murray et al., 2015) have validated its significant importance for surface NO_x as well as O_3 formation, current global chemical transport models (CTMs) usually do not include this emission source (Zatko et al., 2016).

In this study, we employ a global chemical transport model, GEOS-Chem CTM, to evaluate the model performance for surface O_3 and its precursors over Summit, in conjunction with two years in-situ measurements during 2008-2010. This paper is organized as follows: section 2 describes

model methods and observations, followed by detailed comparisons of model simulations against observations for O_3 and O_3 precursors in section 3; conclusions are summarized in section 4.

2. Observational data and model simulations

In situ measurements of NO_x, PAN, and non-methane hydrocarbons (NMHCs) were performed at Summit from July 2008 to June 2010 (Helmig et al., 2014b; Kramer et al., 2015). An automated O_3 chemiluminescence detection system was used to measure NO_x (Ridley and Grahek, 1990); a commercial PAN gas chromatography analyzer (PAN-GC, Metcon, In., Boulder, CO) was employed for the measurement of PAN. Measurements of NMHC relied on an automated GC-Flame Ionization Detection (FID) system. Readers are referred to Kramer et al. (2015) and Helmig et al. (2014b) for the details of the measurement techniques and equipment setup. Surface measurements of O_3 using ultraviolet light absorption at 254 nm (Petropavlovskikh and Oltmans, 2012), and CO by GC (Novellie and Masarie, 2015) are from the National Oceanic and Atmospheric Administration (NOAA). Hourly averaged O_3 and flask sampled CO between July 2008 and June 2010 were downloaded from the NOAA Earth System Research Laboratory (ESRL) Global Monitoring Division (GMD) website (http://www.esrl.noaa.gov/gmd/dv/data/). Vertical ozonesonde data profiles were also downloaded from NOAA ESRL GMD (McClure-Begley et al., 2014).

The GEOS-Chem CTM (Bey et al., 2001) was used to simulate the seasonal cycles of O_3 and related species (NO_x, PAN, NMHCs) at Summit. The GEOS-Chem model has fully coupled O_3-NO_x-VOC-Aerosol chemistry mechanism and is driven by assimilated meteorological data from the Goddard Earth Observing System version 5 (GEOS-5) of the NASA Global Modeling Assimilation Office. The GEOS-Chem model has been extensively evaluated and applied in a wide range of applications (Martin et al., 2002; Park et al., 2004; Wu et al., 2007; Hudman et al., 2009; Johnson et al., 2010; Huang et al., 2013; Kumar et al., 2013; Zhang et al., 2014; Hickman et al., 2017). GEOS-Chem v10-1 with grid resolution of 4˚ latitude by 5˚ longitude, and 47 vertical layers was used for the model control simulation. Following McLinden et al. (2000), the Linoz stratospheric O_3 chemistry scheme was used. The simulation was run from June 2007 to June 2010 and the results from the last two years were used in the final analysis. Time series data were archived with 3-hr temporal resolution at the Summit grid box.

Global anthropogenic emissions of NO_x, SO_2, NH_3, and CO in the model are based on the Emission Database for Global Atmospheric Research (EDGAR) v4.2 inventory, which is overwritten by regional emission inventories where applicable, such as the BRAVO inventory for Mexico (Kuhns et al., 2005), the CAC over Canada, the EMEP emissions over Europe, the Model Inter-comparison Study for Asia Phase III (MIX) emissions over Asia (Li et al., 2017), and the US EPA NEI 2011 (NEI11) emission inventory (Simon et al., 2010). Soil NO_x emission scheme follows Hudman et al. (2012). Lightning NO_x emissions are calculated per flash rate based on GEOS-5 computed cloud-top heights (Price and Rind, 1992), which are determined by deep convection and constrained by satellite observations for monthly average flash rates from the Lightning Imaging Sensor and Optical Transient Detector (OTD/LIS) (Sauvage et al., 2007; Murray et al., 2012). Biomass burning emissions are from the Global Fire Emission Database version 4 (GFED4) inventory with monthly resolution (Giglio et al., 2013). The RETRO global anthropogenic NMHC emission inventory (van het Bolscher et al., 2008) was used except for C_2H_6 and propane (C_3H_8), which follows Xiao et al. (2008, hereafter referred to as X08) for the year 2001. Global biofuel emission inventory follows Yevich and Logan (2003), which includes emissions for C_2H_6 and C_3H_8. For biogenic VOC emissions, the Model of Emissions of Gases and Aerosols from Nature (MEGAN) scheme (Guenther et al., 2006) was used. Dry deposition of species in GEOS-Chem uses a standard resistance-in-series scheme (Wesely, 1989), as implemented in Wang et al. (1998). Wet scavenging follows Liu et al. (2001), including scavenging in convective updraft, rainout (in-cloud) and washout (below-cloud) from convective anvils and large-scale precipitation.

We first ran the standard GEOS-Chem model with a-priori emissions and compare the simulation results against observations for various species (including NO_x, PAN, C_2H_6, C_3H_8, CO, and O_3, as shown in Fig. 1). Then we focus on the model-observation discrepancies, and where applicable, make revisions to the model simulations and further evaluate the improvement in model performance, as discussed in details below.

3. Results and Discussions

3.1 NO_x

We first combine the two years of data for July 2008 – June 2010 and anylaze their seasonal variations. As shown in Figure 1a, the GEOS-Chem model in general captures the abundance and seasonal variation of NO_x for July-October. However, compared to observations the model results significantly (by a factor of 2) overestimate NO_x mixing ratios for November-January, while underestimating the data in spring and early summer by over 50%. Another challenge for the model simulation is that it does not capture the decrease of NO_x for May-December. We find that during the 2009-2010 winter season, model simulations show several high NO_x spikes with peak NO_x mixing ratios reaching ~ 0.15 ppbv or higher, which is ~ 15 times greater than typical backgound levels (Fig. 2). These large peaks in NO_x were not observed in the data. Similar peaks were also seen in the model simulations during the 2008-2009 winter season; however, there are no measurement data available for this period to compare with.

Further analyses show that the model-simulated high NO_x spikes during wintertime are all associated with transport events from Europe. We carried out a sensitivity study to examine the impacts of European emissions on Arctic NO_x by mannually reducing anthropogenic NO_x emissions from the EMEP emission inventory over Europe by 50% (EMEP50). Results show that surface peak NO_x mixing ratios over Summit during the spike events (e.g., dates around 12/09/2009, 12/15/2009, 1/15/2010 and 1/22/2010) from EMEP50 almost decline proportionally by approximately 50% during 2009/12/01-2010/01/31 (Fig. 2), which confirms that the modeled NO_x spikes at Summit during wintertime are associated with transport from Europe. However, the model simulated NO_x is still significantly higher than observations. Comparisons for surface NO_2 mixing ratios between model simulations and 11 in-situ observational sites over Europe during this period were conducted with data downloaded from http://ebas.nilu.no. For detailed site information, NO_2 measurement technique and resolution, refer to Table 1. Measurment data over these two months for each site were averaged to compare with the corresponding grid cell in the model. As shown in Figure 3a, GEOS-Chem overestimates surface NO_2 mixing ratios at these sites by over 66%, compared with observations.

Instead of using EMEP, we carried out another sensitivity study to force anthropogenic NO_x emissions over Europe following EDGAR v4.2 (EURO_EDGAR), with other model configurations identical to control simulations. As shown in Figure 2, the NO_x mixing ratios over Summit during 12/2009-01/2010 agree much better with observations, especially for January

2010 where the model captures the magnitudes of observational peaks (Fig. 2). This is because NO_x emissions from EDGAR over Europe (1.97 Tg NO) are 12% lower than that from EMEP (2.24 Tg NO) for the months of 12/2009 and 01/2010. Furthermore, the discrepancy for the differences of surface NO_2 mixing ratios over Europe between EURO_EDGAR and observations is further reduced (by 50%), relative to the control runs (Fig. 3b). Similarly, we also tested the sensitivty of surface NO_x mixing ratios over Summit in response to the changes in the anthropogenic NO_x emissions from NEI11 over US and MIX over Asia (including Siberia) during these two months, and found that surface NO_x mixing ratio over Summit during these two months were quite close to the control simulations (not shown), reflecting insenstivity to emission perturbations from US and Asia. Therefore, we conclude that uncertainties in fossil fuel NO_x emissions of EMEP associated with transport events from Europe in the model are the most likely cause for the wintertime NO_x spikes over Summit.

For April-July, model simulated monthly mean NO_x mixing ratios over Summit are a factor of two lower than the observations (Fig. 4a). In-situ measurements at Summit by Honrath et al. (1999, 2000a, 2000b, 2002) showed upward fluxes of NO_x (2.52×10^8 molecules cm^{-2} s^{-1}) from photolysis of nitrate in snowpack during the summertime, leading to enhancement in NO_x levels in the surface layer by approximately 20 pptv, which is comparable to surface NO_x mixing ratios in the Arctic from other sources. Similar results were found over the East Antarctic Plateau, a remote Antarctic location (75.1˚ S, 123.3˚ E) covered by snow/ice sheet (Frey et al., 2013; Legrand et al., 2014). The standard GEOS-Chem model does not include the photolysis of nitrate from snowpack, implying a missing source for NO_x in the Arctic/Antarctic boundary layer.

In order to test the sensitivity of model simulated surface NO_x mixing ratios to the snowpack emissions, we implement in the model a constant 24-hr NO_x flux ~ 2.52 x 10^8 molecules cm^{-2} s^{-1} during April-July over Greenland (60-85° N, 20-60° W), following the measurements conducted at Summit during summertime by Honrath et al. (2002). As a result, we find that on average, the model simulated surface NO_x mixing ratios for April to July over Summit are more than double that from the control simulation, which improves the agreement between model and observations (Fig. 4a). However, the model is still not able to reproduce the decreasing trends of NO_x for May-October. This may be caused by the seasonally decreasing NO_x production rate in the

snowpack from spring to fall from a gradual depletion of the snowpack NO_x reservoir (Van Dam et al., 2015), whereas the model considers a simple constant NO_x emission flux.

3.2 PAN

Figure 1b shows the comparison of model simulated monthly mean PAN mixing ratios with the measurement data. The model captures the seasonal variation of PAN well, although significantly (by ~30%) underestimting the PAN mixing ratios for April-June. By running the model simulation with higher horizontal resolution at 2° latitude by 2.5° longitude (hereafter referred to as GEOS-Chem 2x2.5), we find that the monthly mean PAN mixing ratios over Summit during April-July are increased by up to 23.3 pptv compared to the 4x5 simulation (Fig. 4b). This can be explained by two reasons. First, coarse model resolution (e.g., 4x5 horizontal resolution) could artificially smear the intense emission sources throughout the entire grid cell (e.g., over urban regions), leading to underestimates of downwind concentrations for species, e.g., O_3 and O_3 precursors (Jang et al., 1995; Yu et al., 2016). Second, ventilation of lower atmosphere could be better resolved by fine model resolution, leading to more efficient vertical advection (Wang et al., 2004; Chen et al., 2009; Yu et al., 2016). However, on average, monthly mean model simulated PAN mixing ratios are still underestimated by 20% during this period, compared with observations.

Snowpack can emit not only NO_x, but also PAN, based on field studies at Summit during summertime by Ford et al. (2002). GEOS-Chem does not contain snowpack PAN emissions and chemistry. For a sensitivity study, similar to snowpack NO_x emissions as discussed in section 3.1, we considered a 24-hr constant flux of 2.52 x 10^8 molecules cm^{-2} s^{-1} of PAN from April to July, following Ford et al. (2002). As a result, model simulated PAN mixing ratios agree much better with observations (Fig. 4b). Note that there are also other possible reasons that lead to model bias. For instance, a study by Fischer et al. (2014) showed that an improved agreement between modeled and measured PAN in the high latitudes can be found when the model was forced to emit a portion of the fire emissions above the boundary layer as well as by directly partitioning 40% of NO_x emissions from fires into PAN. However, in our case, we did not find much difference beteween a sensitivity study following this method and our control runs.

3.3 NMHC

Comparisons of observed surface C_2H_6 and C_3H_8 mixing ratios with GEOS-Chem simulations at Summit are shown in Figures 1c and d. The model simulations agree well with surface measurements of C_3H_8, but systematically overestimate C_2H_6 (by approximately 25% annually), with the largest bias (0.48 ppbv) occuring during summer. This is consistent with the study from Tzompa-Sosa et al., (2017), which used the same model as our study and pointed out that using X08 as global anthropogenic C_2H_6 emission inventory systematically overestimated surface C_2H_6 mixing ratios over the Northern Hemisphere, compared with ground-based observations. Anthropogenic C_2H_6 emissions over US from NEI11 are shown to geographically match the distribution of active oil and natural wells (Tzompa-Sosa et al., 2017), and the most recent MIX has been updated to synergize anthropogenic C_2H_6 emissions from various countries over Asia (Li et al., 2017). Therefore, instead of using global anthropogenic fossil fuel emissions of C_2H_6 following X08, we first conducted sensitivity simulations by overwritting global emission inventories by NEI11 over US, and MIX over Asia (hereafter referred to as NEI11_MIX). Both NEI11 and MIX contain emissions for the years from 2008 to 2010, which could realistically represent the annual and seasonal variations of C_2H_6 emissions over the US and Asia, thus spatially and temporally better representative of anthropogenic C_2H_6 emissions from mid-latitudes transported to the Arctic regions. In general, model control simulations overestimate annual mean surface C_2H_6 mixing ratios primarily in the Northern Hemisphere, with large differences occurring over Asia and US by up to 5 ppbv, compared with NEI11_MIX during the period of 07/2008-06/2010 (Fig. S1). All the above changes are driven by the substantial reductions of anthropogenic C_2H_6 emissions between emission inventories, from 3.5 (X08) to 2.5 Tg/yr (MIX) over Asia, and from 1.9 Tg/yr (X08) to 1.4 Tg/yr (NEI11) over US, reflecting decreasing trend of anthropogenic C_2H_6 emissions during 2001-2009 because X08 emission inventory is based on the year 2001, which is consistent with Helmig et al. (2014a). Substantial changes in surface C_2H_6 mixing ratios over the US bewteen control simulations and NEI11_MIX reflects that there exist tempospatial changes of C_2H_6 emissions from oil and gas productions during the period of 2001-2009. A similar pattern was also found by Tsompa-Sosa et al. (2017). In contrast to the control simulations, NEI11_MIX model simulations show that monthly mean C_2H_6 mixing ratios over Summit are systematically underestimated by 24%, compared with observations (Fig. 5). Tsompa-Sosa et al. (2017) reported that NEI11 for C_2H_6 emissions were likely underestimated by 40%, compared with in-situ and aircraft observations over the US. With

NEI11 C_2H_6 emissions increases by 40%, however, model simulated annual mean C_2H_6 mixing ratios over Summit only increase by 6% during the period of 07/2008-06/2010, relative to NEI11_MIX.

Similar to NEI11_MIX, we further conducted sensitivity studies by only replacing the regional emission inventory for C_2H_6 over the US, with other regions still following X08 (hereafter referred to as NEI11_ONLY). Consequently, model simulated surface C_2H_6 mixing ratios over Summit agree better with observations during winter-spring (Fig. 5), decreasing the bias from +15% (control simulations) to +6%. However, model simulated C_2H_6 mixing ratios during summer-fall are higher than the observations by over 30%.

We then scaled up the MIX emissions for C_2H_6 by 20% over Asia, with other model configurations identical to NEI11_MIX (hereafter referred to as NEI11_MIX20). By doing this, we increase fossil fuel C_2H_6 emissions from 2.5 to 3 Tg/yr. We find that annual mean C_2H_6 mixing ratios from NEI11_MIX20 agree quite well with observations over Summit, with bias less than 1% (Fig. 5). This implies that further assessments of anthropogenic C_2H_6 emissions from MIX over Asia are needed and a more accurate global anthropogenic C_2H_6 emission inventory should be developed and validated to replace X08 in the future. Note that this standard version of GEOS-Chem does not account for the sink of C_2H_6 from the reaction with chlorine, which could reduce the global annual mean surface C_2H_6 mixing ratios by 0-30%, and the global burden of C_2H_6 by about 20%, compared with the simulation without considering the halogen chemistry (Sherwen et al., 2016), which introduces additional uncertainty for our measurement-model comparison, together with the highly uncertain seasonality of C_2H_6 chemistry.

3.4 CO

Figure 1e shows the comparison of model simulated CO mixing ratios with observations over Summit. Overall, the model generally captures the seasoanl trend and annual mean of CO, with annual mean model simulated CO mixing ratios slightly overestimated by up to 3 ppbv, compared with observations.

3.5 O_3

Surface O_3 mixing ratios from model simulations and surface observations are compared in Figure 1f. The GEOS-Chem model captures the seasonal variation of O_3 including the spring peak. However, the model shows a systematic low bias for most time of the year, in particualr for April–July when the surface O_3 mixing ratios are underestimated by approximately 13% (~ 6.5 ppbv). Here we focus our analysis for the possible causes that lead to the model low bias during April-July.

As discussed earlier, snowpack emissions due to the photolysis of nitrate in the snow during late spring and summer could contribute to NO_x and HONO levels in the ambient air which could significantly enhance O_3 production (Crawford et al., 2001; Zhou et al., 2001; Dibb et al., 2002; Honrath et al., 2002; Yang et al., 2002; Grannas et al., 2007; Helmig et al., 2008; Legrand et al., 2014). We ran a sensitivity study to test the response of surface O_3 mixing ratios to the perturbations of NO_x and HONO from snowpack emissions. In addtion to snowpack NO_x emissions that are described in Section 3.1, we implemented in the model a constant flux of HONO (4.64 x 10^7 molecules cm^{-2} s^{-1}) from April to July over Summit as well (Honrath et al., 2002). As a result, monthly mean model simulated surface O_3 mixing ratios increase by up to 3 ppbv during this period (Fig. 6). The largest effect occurs in July due to relatively strong solar radiation. O_3 formation due to snowpack emissions in our study is slightly higher than that in Zatko et al. (2016) because HONO from snowpack emissions is not considered in their study. However, for the months of April and May, surface O_3 mixing ratios only increase by ~ 1 ppbv, compared with the control runs. That is, even after accounting for the snowpack emissions, the model simulated O_3 mixing ratios are still significantly lower than the observations.

Comparison of the model simulations with different resolutions (4x5 vs. 2x2.5) shows that the finer resolution simulations substantially increase monthly mean O_3 mixing ratios over Summit by up to 6 ppbv for the months of June and July (Fig. 6). As discussed in section 3.2, fine model resolution can better resolve the emission strengths, which could significantly affect downwind chemical reactions, e.g., O_3 production efficiency (Liang and Jacobson, 2000). Moreover, terrain elevations from fine model resolution are better represented (thus better representative of Summit's elevation) and more efficient vertical ventilation of O_3 and O_3 precursors can be achieved (Wang et al., 2004). Together with the impact of snowpack chemistry, this brings model simulated surface O_3 mixing ratios over Summit in much better agreement with

observations for these two months. Unfortunately, there is still a low bias in the model for the months of April and May.

Another possible cause for the O_3 biases between model simulations and observations is the stratosphere-to-troposphere exchange scheme (STE) in the model for O_3. Liang et al. (2011) have pointed out that STE could be a significant direct sources of O_3 in the Arctic during spring-summer. We retrieved vertical profiles of O_3 mixing ratios and specific humidity from ozonesondes (0-5 km elevation above the Summit surface) launched at Summit for the months of June and July in 2008 and compared those data with model control runs. Ozonesondes were launched intensively during these two months (a total of 19 times). As shown in Figure 7, compared with observations, model simulated O_3 mixing ratios averaged over 0-5 km above the ground level are underestimated by 3% and 9% in June and July 2008 (Fig. 7a). However, specific humidity in GEOS-5 is overestimated by 50% and 81% (Fig. 7b) respectively. Ozonesonde data show that Summit frequently encounters high O_3/low water vapors events (e.g., July 9-11, 2008), which are likely of upper tropospheric/stratospheric origins (Helmig et al., 2007b), but these are not captured by the model, which implies that GEOS-Chem possibly underestimates STE for O_3 over Summit.

Boundary layer height is another factor that could potentially affect the discrepancy of O_3 mixing ratios between model and observations. The mean springtime afternoon (12:00-14:00, local time) boundary layer height in the model at Summit for the year 2009 is 160 m, which agrees fairly well with observations (156 m) at Summit conducted in spring 2005 (Cohen et al., 2007). Therefore, we exclude that model uncertainties in boundary layer height representation in springtime cause the low bias of O_3 mixing ratios between model and observations.

Lastly, we also compared O_3 dry deposition velocity (V_{dry}) in the model in springtime with observations at Summit. For spring 2009, mean O_3 V_{dry} in the model at Summit is 0.009 cm s^{-1}, which is within the range of -0.01-0.01 cm s^{-1} observed at Summit (Helmig et al., 2009). Helmig et al. (2009) revealed that afternoon (12:00-18:00, local time) O_3 V_{dry} during springtime was close to 0.01 cm s^{-1}. For other times during the day, O_3 V_{dry} was either close to zero or negative (i.e., O_3 production over the snow outweighs its dry deposition). As a result, the net mean O_3 V_{dry} from observations during springtime is about 4-6 times lower than model simulations. Therefore,

model overestimation of O_3 loss via surface uptake is another factor that contributes to the low bias of surface O_3 mixing ratios at Summit in the model during springtime.

4. Conclusions

We combine model simulations with two-year (July 2008-June 2010) ground based measurements at Summit to better understand the abundance and seasonal variations of tropospheric O_3 and related species in the Arctic. In general, the GEOS-Chem model is capable of reproducing the seasonal cycles of NO_x, PAN, C_2H_6, C_3H_8, CO, and O_3. However, some major discrepancies between model and observations, especially for NO_x, PAN, C_2H_6, and O_3 are also identified.

There are significant differences between model simulated NO_x mixing ratios and observations for the spring and winter seasons. The model underestimates NO_x mixing ratios by approximately 50% during late spring to early summer, which is likely due to the missing NO_x emissions from nitrate photolysis in the snowpack. At the same time, the model overestimates NO_x mixing ratios by more than a factor of two in wintertime. Model simulations indicate episodic but frequent transport events from Europe in wintertime leading to NO_x spikes reaching 15 times typical NO_x mixing ratios at Summit; these large NO_x spikes are not seen in the observational data. We have carried out multiple sensitivity model studies but are still unable to reconcile this discrepancy.

The model successfully captures the seasonal cycles and the spring maximum PAN mixing ratios, although it underestimates PAN by over 30% during late spring and early summer. Model sensitivity studies reveal that this discrepancy could be largely resolved by accounting for PAN emissions from snowpack.

For C_3H_8 and CO, model simulations overall agree well with the surface measurements, however, the model tends to systematically overestimate surface C_2H_6 mixing ratios by approximately 20% on an annual average, compared with observations. This may be explained by that annual emission budgets of C_2H_6 over US and Asia from X08 emission inventory are higher than those from NEI11 and MIX by over 40%. By replacing X08 over US with NEI11 for C_2H_6, and scaling up MIX by 20%, the model-observation bias can be resolved, with annual mean bias less than 1%. However, care must be taken to interpret this result because we do not

take into account other factors that may influence the discrepancy of surface C_2H_6 mixing ratios at Summit between model and observations, such as the C_2H_6 chemistry with cholorine.

GEOS-Chem is able to reproduce the seasonal variation of surface O_3 at Summit but persistently underestimates O_3 mixing ratios by approximately 13% (~ 6.5 ppbv) from April to July. This low bias is likely caused by a combination of misrepresentations, including the missing snowpack emissions of NO_x and HONO, inaccurate representation of Summit's elevation from coarser model resolutions, model overestimated O_3 dry deposition velocity during springtime, as well as the underestimated STE.

All the results presented above reveal the importance of local snowpack emissions in regulating the air quality over Arctic. Improvements in global CTM could likely be achieved by coupling snowpack emissions of reactive gases and photochemistry modules in order to better simulate O_3 and O_3 precursors over snow and ice in the Arctic (Zatko et al., 2016). Moreover, this study also demonstrates that anthropogenic emissions from midlatitudes play an important role in affecting the Arctic air quality. However, further investigations in anthropogenic NO_x emissions over Europe and C_2H_6 emissions over Asia and North America are needed. The uncertainties in O_3 dry deposition and STE scheme in GEOS-Chem are warranted to be better quantified in our future study.

Acknowledgements This research was funded by U.S. EPA grant 83518901). Its contents are solely the responsibility of the grantee and do not necessarily represent the official views of the U.S. EPA. Further, U.S. EPA does not endorse the purchase of any commercial products or services mentioned in the publication. Superior, a high performance computing cluster at Michigan Technological University, was used in obtaining results presented in this publication. L. J. Kramer, D. Helmig and R. E. Honrath thank NASA (grant NNX07AR26G) for supporting the measurements at Summit. We acknowledge the observational dataset of O_3 and CO provided by NOAA ESRL. Technical supports from M. Sulprizio and C. Keller are also acknowledged.

References

Alvarado, M. J., Logan, J. A., Mao, J., Apel, E., Riemer, D., Blake, D., Cohen, R. C., Min, K.-E., Perring, A. E., Browne, E. C., Wooldridge, P. J., Diskin, G. S., Sachse, G. W., Fuelberg, H., Sessions, W. R., Harrigan, D. L., Huey, G., Liao, J., Case-Hanks, A., Jimmenez, J. L., Cubison, M. J., Vay, S. A., Weinheimer, A. J., Knapp, D. J., Montzka, D. D., Flocke, F. M., Pollack, I. B., Wennberg, P. O., Kurten, A., Crounse, J., St. Clair, J. M., Wisthaler, A., Mikoviny, T., Yantosca, R. M., Carouge, C. C., and Le Sager, P.: Nitrogen oxides and PAN in plumes from boreal fires during ARCTAS-B and their impact on ozone: an integrated analysis of aircraft and satellite observations, Atmos. Chem. Phys., 10, 9739-9760, doi:10.5194/acp-10-9739-2010, 2010.

Aydin, M., Verhulst, K. R., Saltzman, E. S., Battle, M. O., Montzka, S. A., Blake, D. R., Tang, Q., and Prather, M. J.: Recent decreases in fossil-fuel emissions of ethane and methane derived from firn air, Nature, 476, 198–201, doi:10.1038/nature10352, 2011.

Bey, I., Jacob, D. J., Yantosca, R. M., Logan, J. A., Field, B. D., Fiore, A. M., Li, Q., Liu, H., Mickley L. J., and Schultz, M. G.: Global modeling of tropospheric chemistry with assimilated meteorology: Model description and evaluation, J. Geophys. Res.-Atmos., 106, 23073-23095, 2001.

Blake, D. R., and Rowland, F. S.: Global atmospheric concentrations and source strength of ethane, Nature, 321, 231–233, 1986.

Chen, D., Wang, Y., McElroy, M. B., He, K., Yantosca, R. M., and Le Sager, P.: Regional CO pollution and export in China simu- lated by the high-resolution nested-grid GEOS-Chem

model, Atmos. Chem. Phys., 9, 3825–3839, doi:10.5194/acp-9-3825-2009, 2009.

Cohen, L., Helmig, D., Neff, W., Grachev, A., and Fairall, C.: Boundary-layer dynamics and its influence on atmospheric chemistry at Summit, Greenland, Atmos. Environ., 41, 5044–5060, 2007.

Crawford, J. H., Davis, D. D., Chen, G., Buhr, M., Oltmans, S., Weller, R., Mauldin, L., Eisele, F., Shetter, R., Lefer, B., Ari- moto, R., and Hogan, A.: Evidence for photochemical production of ozone at the South Pole surface, Geophys. Res. Lett., 28, 3641–3644, 2001.

Dibb, J. E., Arsenault, M., Peterson, M. C., and Honrath, R. E.: Fast nitrogen oxide photochemistry in Summit, Greenland snow, Atmospheric Environment, 36, 2501-2511, 2002.

Emmons, L. K., Arnold, S. R., Monks, S. A., Huijnen, V., Tilmes, S., Law, K. S., Thomas, J. L., Raut, J.-C., Bouarar, I., Turquety, S., Long, Y., Duncan, B., Steenrod, S., Strode, S., Flemming, J., Mao, J., Langner, J., Thompson, A. M., Tarasick, D., Apel, E. C., Blake, D. R., Cohen, R. C., Dibb, J., Diskin, G. S., Fried, A., Hall, S. R., Huey, L. G., Weinheimer, A. J., Wisthaler, A., Mikoviny, T., Nowak, J., Peischl, J., Roberts, J. M., Ryerson, T., Warneke, C., and Helmig, D.: The POLARCAT Model Intercomparison Project (POLMIP): overview and evaluation with observations, Atmos. Chem. Phys., 15, 6721–6744, doi:10.5194/acp-15-6721-2015, 2015.

Etiope, G., and Ciccioli, P.: Earth's degassing: A missing ethane and propane source, Science, 323, 1, 2009.

Fiore, A. M., Jacob, D. J., Field, B. D., Streets, D. G., Fernandes, S. D., and Jang, C.: Linking

ozone pollution and climate change: The case for controlling methane, Geophys. Res. Lett., 29, 1919, doi:10.1029/2002GL015601, 2002.

Fischer, E. V., Jacob, D. J., Yantosca, R. M., Sulprizio, M. P., Millet, D. B., Mao, J., Paulot, F., Singh, H. B., Roiger, A., Ries, L., Talbot, R. W., Dzepina, K., and Pandey Deolal, S.: Atmospheric peroxyacetyl nitrate (PAN): a global budget and source attribution, Atmos. Chem. Phys., 14, 2679-2698, doi:10.5194/acp-14-2679-2014, 2014.

Ford, K. M., Shepson, P. B., Bertman, S. B., Honrath, R. E., Peterson, M., Dibb, J. E., and Bottenheim, J. W.: Studies of peroxyacetyl nitrate (PAN) and its interaction with the snowpack at Summit, Greenland, J. Geophys. Res., 107, ACH6, doi:10.1029/2001JD000547, 2002.

Franco, B., Bader, W., Toon, G., Bray, C., Perrin, A., Fischer, E., Sudo, K., Boone, C., Bovy, B., Lejeune, B., Servais, C., and Mahieu, E.: Retrieval of ethane from ground-based FTIR solar spectra using improved spectroscopy: Recent burden increase above Jungfraujoch, J. Quant. Spectrosc. Ra., 160, 36–49, doi:10.1016/j.jqsrt.2015.03.017, 2015.

Franco, B., Mahieu, E., Emmons, L. K., Tzompa-Sosa, Z. A., Fischer, E. V., Sudo, K., Bovy, B., Conway, S., Griffin, D., Hannigan, J. W., Strong, K., and Walker, K. A.: Evaluating ethane and methane emissions associated with the development of oil and natural gas extraction in North America, Environ. Res. Lett., 11, doi:10.1088/1748-9326/11/4/044010, 2016.

Frey, M. M., Brough, N., France, J. L., Anderson, P. S., Traulle, O., King, M. D., Jones, A. E., Wolff, E. W., and Savarino, J.: The diurnal variability of atmospheric nitrogen oxides (NO and NO_2) above the Antarctic Plateau driven by atmospheric stability and snow emissions, Atmos.

Chem. Phys., 13, 3045-3042, doi:10.5194/acp-13-3045-2013, 2013.

Giglio, L., Randerson, J. T., and van der Werf, G. R.: Analysis of daily, monthly, and annual burned area using the fourth-generation global fire emissions database (GFED4), J. Geophys. Res. Biogeosci., 118, 1, 317-328, doi:10.1002/jgrg.20042, 2013.

Grannas, A. M., Jones, A. E., Dibb, J., Ammann, M., Anastasio, C., Beine, H. J., Bergin, M., Bottenheim, J., Boxe, C. S., Carver, G., Chen, G., Crawford, J. H., Domine, F., Frey, M. M., Guzman, M. I., Heard, D. E., Helmig, D., Hoffmann, M.R., Honrath, R. E., Huey, L. G., Hutterli, M., Jacobi, H. W., Klán, P., Lefer, B., McConnell, J., Plane, J., Sander, R., Savarino, J., Shepson, P. B., Simpson, W. R., Sodeau, J. R., von Glasow, R., Weller, R., Wolff, E. W., and Zhu, T.: An overview of snow photochemistry: evidence, mechanisms and impacts, Atmos. Chem. Phys., 7, 4329–4373, doi:10.5194/acp-7-4329-2007, 2007.

Guenther, A., Karl, T., Harley, P., Wiedinmyer, C., Palmer, P. I., and Geron C.: Estimate of global terrestrial isoprene emissions using MEGAN (Model of Emissions of Gases and Aerosols from Nature), Atmos. Chem. Phys., 6, 3181-3210, doi:10.5194/acp-6-3181-2006, 2006.

Gupta, M. L., Cicerone, R. J., Blake, D. R., Rowland, F. S., and Isaksen, I. S. A.: Global atmospheric distributions and source strengths of light hydrocarbons and tetrachloroethene, J. Geophys. Res., 103, 28219–28235, 1998.

Hausmann, P., Sussmann, R., and Smale, D.: Contribution of oil and natural gas production to renewed increase in atmo- spheric methane (2007–2014): top–down estimate from ethane and methane column observations, Atmos. Chem. Phys., 16, 3227–3244, doi:10.5194/acp-16-

3227-2016, 2016.

Helmig, D., Oltmans, S. J., Carlson, D., Lamarque, J. F., Jones, A., Labuschagne, C., Anlauf, K., Hayden, K.: A review of surface ozone in the polar regions, Atmospheric Environment, 41, 5138-5161, 2007a.

Helmig, D., Oltmans, S. J., Morse, T. O., and Dibb, J. E.: What is causing high ozone at Summit, Greenland?, Atmos. Environ., 41, 5031-5043, doi:10.1016/j.atmosenv.2006.05.084, 2007b.

Helmig, D., Ganzeveld, L., Butler, T., and Oltmans, S. J.: The role of ozone atmosphere-snow gas exchange on polar, boundary–layer tropospheric ozone- a review and sensitivity analysis, Atmos. Chem. Phys., 7, 15-30, doi:10.5194/acp-7-15-2007, 2007c.

Helmig, D., Johnson, B., Oltmans, S. J., Neff, W., Eisele, F., and Davis, D. D.: Elevated ozone in the boundary-layer at South Pole, Atmos. Environ., 42, 2788–2803, 2008.

Helmig, D., Cohen, L. D., Bocquet, F., Oltmans, S., Grachev, A., and Neff, W.: Spring and summertime diurnal surface ozone fluxes over the polar snow at Summit, Greenland, Geophys. Res. Lett., 36, L08809, doi:10.1029/2008GL036549, 2009.

Helmig, D., Petrenko, V., Martinerie, P., Witrant, E., Röckmann, T., Zuiderweg, A., Holzinger, R., Hueber, J., Thompson, C., White, J. W. C., Sturges, W., Baker, A., Blunier, T., Etheridge, D., Rubino, M., and Tans, P.: Reconstruction of Northern Hemisphere 1950–2010 atmospheric non-methane hydrocarbons, Atmos. Chem. Phys., 14, 1463–1483, doi:10.5194/acp-14-1463-2014, 2014a.

Helmig, D., Stephens, C., Caramore, J., and Hueber, J.: Seasonal behavior of non-methane hydrocarbons in the firn air at Summit, Greenland, Atmos. Environ., 85, 234-246,

doi:10.1016/j.atmosenv.2013.11.021, 2014b.

Helmig, D., Rossabi, S., Hueber, J., Tans, P., Montzka, S. A., Masarie, K., Thoning, K., Plass-Duelmer, C., Claude, A., Car- penter, L. J., Lewis, A. C., Punjabi, S., Reimann, S., Vollmer, M. K., Steinbrecher, R., Hannigan, J. W., Emmons, L. K., Mahieu, E., Franco, B., Smale, D., and Pozzer, A.: Reversal of global atmospheric ethane and propane trends largely due to US oil and natural gas production, Nat. Geosci., 9, 490–495, doi:10.1038/ngeo2721, 2016.

Hickman, J. E., Huang, Y., Wu, S., Diru, W., Groffman, P. M., Tully, K. L., and Palm, C. A.: Nonlinear response of nitric oxide fluxes to fertilizer inputs and the impacts of agricultural intensification on tropospheric ozone pollution in Kenya, Glob. Change Biol., 23, 3193-3204, doi:10.1111/gcb.13644, 2017.

Hollaway, M. J., Arnold, S. R., Challinor, A. J., and Emberson, L. D.: Intercontinental trans-boundary contributions to ozone-induced crop yild losses in the North Hemisphere, Biogeosciences, 9, 271-292, doi: 10.5194/bg-9-271-2012, 2012.

Honrath, R. E., Peterson, M. C., Guo, S., Dibb, J. E., Shepson, P. B., and Campbell, B.: Evidence of NO_x production within or upon ice particles in the Greenland snowpack, Geophys. Res. Lett., 26, 695-698, 1999.

Honrath, R. E., Guo, S., Peterson, M. C., Dziobak, M. P., Dibb, J. E., and Arsenault, M. A.: Photochemical production of gas phase NO_x from ice crystal NO_3^-, J. Geophys. Res., 105, 24183–24190, 2000a.

Honrath, R. E., Peterson, M. C., Dziobak, M. P., Dibb, J. E., Arsenault, M. A., and Green, S. A.: Release of NO_x from Sunlight-irradiated Midlatitude Snow, Geophys. Res. Lett., 27, 2237–2240, 2000b.

Honrath, R. E., Lu, Y., Peterson, M. C., Dibb, J. E., Arsenault, M. A., Cullen, N. J., and Steffen, K.: Vertical fluxes of NO_x, HONO, and HNO_3 above the snowpack at Summit, Greenland, Atmos. Environ., 36, 2629-2640, doi:10.1016/S1352-2310(02)00132-2, 2002.

Huang, Y., Wu, S., Dubey, M. K., and French, N. H. F.: Impact of aging mechanism on model simulated carbonaceous aerosols, Atmos. Chem. Phys., 13, 6329–6343, doi:10.5194/acp-13-6329-2013, 2013.

Hudman, R. C., Moore, N. E., Mebust, A. K., Martin, R. V., Russell, A. R., Valin, L. C., and Cohen, R. C.: Steps towards a mechanistic model of global soil nitric oxide emissions: implementation and space based-constraints, Atmos. Chem. Phys., 12, 7779-7795, doi: 10.5194/acp-12-7779- 2012, 2012.

Hudman, R. C., Murray, L. T., Jacob, D. J., Turquety, S., Wu, S., Millet, D. B., Avery, M., Goldstein, A. H., and Holloway, J.: North American influence on tropospheric ozone and the effects of recent emission reductions: Constraints from ICARTT observations, J. Geophys. Res., 114, D07302, doi:10.1029/2008JD010126, 2009.

Jacob, D. J., Wofsy, S. C., Bakwin, P. S., Fan, S.-M., Harriss, R. C., Talbot, R. W., Bradshaw, J. D., Sandholm, S. T., Singh, H. B., Browell, E. V., Gregory, G. L., Sachse, G. W., Shipham, M. C., Blake, D. R., and Fitzjarrald, D. R.: Summertime photochemistry of the troposphere at high northern latitudes, J. Geophys. Res., 97, D15, 16421-16431, doi:10.1029/91JD01968, 1992.

Jang, J.-C., Jeffries, H., Byun, D., and Pleim, J.: Sensitivity of ozone to model grid resolution – I. Application of high resolution regional acid deposition model, Atmos. Environ., 29, 3085-3100, doi:10.1016/1352-2310(95)00118-I, 1995.

Johnson, M.S., Meskhidze, N., Solmon, F., Gasso, S., Chuang, P. Y., Gaiero, D. M., Yantosca, R. M., Wu, S., Wang, X., Carouge, C.: Modeling Dust and Soluble Iron Deposition to the South Atlantic Ocean, J. Geophys. Res., 115, D15202, doi:10.1029/2009JD013311, 2010.

Kanakidou, M., Singh, H. B., Valentin, K. M., and Crutzen, P. J.: A two-dimensional study of ethane and propane oxidation in the troposphere, J. Geophys. Res., 96, 15, 395–315, 413, doi:10.1029/91JD01345, 1991.

Knowlton, K, Rosenthal, J. E., Hogrefe, C., Lynn, B., Gaffin, S., Goldberg, R., Rosenzweig, C., Civerolo, K., Ku, J. Y., Kinney, P. L.: Assessing ozone-related health impacts under a changing climate, Environ. Health Persp., 112, 1557–1563, 2004.

Kramer, L. J., Helmig, D., Burkhart, J. F., Stohl, A., Oltmans, S., and Honrath, R. E.: Seasonal variability of atmospheric nitrogen oxides and non-methane hydrocarbons at the GEOSummit station, Greenland, Atmos. Chem. Phys., 15, 6827-6849, doi:10.5194/acp-15-6827-2015, 2015.

Kuhns, H., Knipping, E. M., and Vukovich, J. M.: Development of a United States-Mexico emissions inventory for the Big Bend Regional Aerosol and Visibility Observational (BRAVO) Study, JAPCA J. Air Waste M., 55, 677–692, 2005.

Kumar, A., Wu, S., Weise, M. F., Honrath, R., Owen, R. C., Helmig, D., Kramer, L., Val Martin, M., and Li, Q.: Free-troposphere ozone and carbon monoxide over the North Atlantic for 2001–2011, Atmos. Chem. Phys., 13, 12537-12547, doi:10.5194/acp-13-12537-2013, 2013.

Legrand, M., Preunkert, S., Frey, M., Bartels-Rausch, Th., Kukui, A., King, M. D., Savarino, J., Kerbrat, M., and Jourdain, B.: Large mixing ratios of atmospheric nitrous acid (HONO) at

Concordia (East Antarctic Plateau) in summer: a strong source from surface snow?, Atmos. Chem. Phys., 14, 9963-9976, doi:10.5194/acp-14-9963-2014, 2014.

Li, M., Zhang, Q., Kurokawa, J., Woo, J. H., He, K. B., Lu, Z., Ohara, T., Song, Y., Streets, D. G., Carmichael, G. R., Cheng, Y. F., Hong, C. P., Huo, H., Jiang, X. J., Kang, S. C., Liu, F., Su, H., and Zheng, B.: MIX: a mosaic Asian anthropogenic emission inventory under the international collaboration framework of the MICS-Asia and the HTAP, Atmos. Chem. Phys., 17, 935-963, doi:10.5194/acpd-17-935-2017.

Liang, J., and Jacobson, M. Z.: Effects of subgrid segregation on ozone production efficiency in a chemical model, Atmos. Environ., 34, 2975–2982, doi:10.1016/S1352-2310(99)00520-8, 2000.

Liang, Q., Rodriguez, J. M., Douglass, A. R., Crawford, J. H., Olson, J. R., Apel, E., Bian, H., Blake, D. R., Brune, W., Chin, M., Colarco, P. R., da Silva, A., Diskin, G. S., Duncan, B. N., Huey, L. G., Knapp, D. J., Montzka, D. D., Nielsen, J. E., Pawson, S., Riemer, D. D., Weinheimer, A. J., and Wisthaler, A.: Reactive nitrogen, ozone and ozone production in the Arctic troposphere and the impact of stratosphere-troposphere exchange, Atmos. Chem. Phys., 11, 13181-13199, doi:10.5194/acp-11-13181-2011, 2011.

Liu, H. Y., Jacob, D. J., Bey, I., and Yantosca, R. M.: Constraints from pb-210 and Be-7 on wet deposition and transport in a global three-dimensional chemical tracer model driven by assimilated meteorological fields, J. Geophys. Res.-Atmos., 106, 12109-12128, doi: 10.1029/2000JD900839, 2001.

Martin, R. V., Jacob, D. J., Logan, J. A., Bey, I., Yantosca, R. M., Staudt, A. C., Li, Q., Fiore, A.

M., Duncan, B. N., and Liu, H.: Interpretation of TOMS observations of tropical tropospheric ozone with a global model and in situ observations, J. Geophys. Res., 107(D18), ACH 4-1-ACH 4-27, doi: 10.1029/2001JD001480, 2002.

McClure-Begley, A., Petropavlovskikh, I., Oltmans, S.: NOAA Global Monitoring Surface Ozone Network. 1973-2014. National Oceanic and Atmospheric Administration, Earth Systems Research Laboratory Global Monitoring Division. Boulder, CO. DATE ACCESSED: 4/23/2017, http://dx.doi.org/10.7289/V57P8WBF, 2014.

McLinden, C. A., Olsen, S. C., Hannegan, B., Wild, O., Prather, M. J., and Sundet, J.: Stratospheric ozone in 3-D models: A simple chemistry and the cross-tropopause flux, J. Geophys. Res., 105, D11, 14653-14665, doi:10.1029/2000JD900124, 2000.

Monks, S. A., Arnold, S. R., Emmons, L. K., Law, K. S., Turquety, S., Duncan, B. N., Flemming, J., Huijnen, V., Tilmes, S., Langner, J., Mao, J., Long, Y., Thomas, J. L., Steenrod, S. D., Raut, J. C., Wilson, C., Chipperfield, M. P., Diskin, G. S., Weinheimer, A., Schlager, H., and Ancellet, G.: Multi-model study of chemical and physical controls on transport of anthropogenic and biomass burning pollution to the Arctic, Atmos. Chem. Phys., 15, 3575-3603, doi:10.5194/acp-15-3575-2015, 2015.

Murray, K. A., Kramer, L. J., Doskey, P. V., Ganzeveld, L., Seok, B., Van Dam, B., and Helmig, D.: Dynamics of ozone and nitrogen oxides at Summit, Greenland. II. Simulating snowpack chemistry during a spring high ozone event with a 1-D process-scale model, Atmos. Environ., 117, 110–123, doi:10.1016/j.atmosenv.2015.07.004, 2015.

Murray, L. T., Jacob, D. J., Logan, J. A., Hudman, R. C., and Koshak, W. J.: Optimized regional

and interannual variability of lightning in a global chemical transport constrained by LIS/OTD satellite data, J. Geophys. Res., 117, D20307, doi:10.1029/2012JD017934, 2012.

Novelli, P. C. and Masarie, K. A.: Atmospheric Carbon Monoxide Dry Air Mole Fraction from the NOAA ESRL Carbon Cycle Cooperative Global Air Sampling Network, 1988-2014, Version: 2015-08-04, NOAA, available at ftp://aftp.cmdl.noaa.gov/data/trace_gases/co/flask/surface/, 2015.

Park, R. J., Jacob, D. J., Field, B. D., Yantosca, R. M., and Chin, M.: Natural and transboundary pollution influences on sulfate-nitrate-ammonium aerosols in the United States: Implications for policy, J. Geophys. Res.-Atmos., 109, D15204, doi:10.1029/2003JD004473, 2004.

Petropavlovskikh, I. and Oltmans, S. J.: Tropospheric Ozone Measurements, 1973-2011, Version: 2012-07-10, NOAA, available at: ftp://aftp.cmdl.noaa.gov/data/ozwv/SurfaceOzone/, 2012.

Pozzer, A., Pollmann, J., Taraborrelli, D., Jöckel, P., Helmig, D., Tans, P., Hueber, J., and Lelieveld, J.: Observed and simulated global distribution and budget of atmospheric C2–C5 alkanes, Atmos. Chem. Phys., 10, 4403–4422, doi:10.5194/acp-10-4403-2010, 2010.

Price, C. and Rind, D.: A simple lightning parameterization for calculating global lightning distributions, J. Geophys. Res., 97, 9919-9933, doi:10.1029/92JD00719,1992.

Ridley, B. A., and Grahek, F.: A small, low flow, high sensitivity reaction vessel for NO chemiluminescence detectors, Am. Meteorol. Soc., 7, 307-311, 1990.

Rudolph, J.: The tropospheric distribution and budget of ethane, J. Geophys. Res., 100, D6, 11369-11381, 1995.

Sauvage, B., Martin, R. V., van Donkelaar, A., Liu, X., Chance, K., Jaeglé, L., Palmer, P. I., Wu, S., and Fu, T.-M.: Remote sensed and in situ constraints on processes affecting tropical tropospheric ozone, Atmos. Chem. Phys., 7, 815–838, doi:10.5194/acp-7-815-2007, 2007.

Sherwen, T., Schmidt, J. A., Evans, M. J., Carpenter, L. J., Groß- mann, K., Eastham, S. D., Jacob, D. J., Dix, B., Koenig, T. K., Sinreich, R., Ortega, I., Volkamer, R., Saiz-Lopez, A., Prados-Roman, C., Mahajan, A. S., and Ordóñez, C.: Global impacts of tropospheric halogens (Cl, Br, I) on oxidants and composi- tion in GEOS-Chem, Atmos. Chem. Phys., 16, 12239–12271, doi:10.5194/acp-16-12239-2016, 2016.

Shindell, D. T., Chin, M., Dentener, F., Doherty, R. M., Faluvegi, G., Fiore, A. M., Hess, P., Koch, D. M., MacKenzie, I. A., Sanderson, M. G., Schultz, M., Stevenson, D. S., Teich, H., Textor, C., Wild, O., Bergmann, D. J., Bey, I., Bian, H., Cuvelier, C., Duncan, B. N., Folberth, G., Horowitz, L. W., Jonson, J., Kaminski, J. W., Marmer, E., Park, R., Pringle, K. J., Schroeder, S., Szopa, S., Takemura, T., Zeng, G., Keating, T. J., and Zuber, A.: A multi-model assessment of pollution transport to the Arctic, Atmos. Chem. Phys., 8, 5353-5372, doi:10.5194/acp-8-5353-2008, 2008.

Simon, H., Beck, L., Bhave, P. V., Divita, F., Hsu, Y., Luecken, D., Mobley, J. D., Pouliot, G. A., Reff, A., Sarwar, G., and Strum, M.: The development and uses of EPA's SPECIATE database, Atmospheric Pollution Research, 196-206, 10.5094/apr.2010.026, 2010.

Simpson, I. J., Sulbaek Andersen, M. P., Meinardi, S., Bruhwiler, L., Blake, N. J., Helmig, D., Rowland, F. S., and Blake, D. R.: Long-term decline of global atmospheric ethane concentrations and implications for methane, Nature, 488, 490–494, doi:10.1038/nature11342,

2012.

Thomas, J. L., Stutz, J., Lefer, B., Huey, L. G., Toyota, K., Dibb, J. E., and von Glasow, R.: Modeling chemistry in and above snow at Summit, Greenland – Part 1: Model description and results, Atmos. Chem. Phys., 11, 4899–4914, doi:10.5194/acp-11-4899- 2011, 2011.

Thomas, J. L., Dibb, J. E., Huey, L. G., Liao, J., Tanner, D., Lefer, B., von Glasow, R., and Stutz, J.: Modeling chemistry in and above snow at Summit, Greenland – Part 2: Impact of snowpack chemistry on the oxidation capacity of the boundary layer, Atmos. Chem. Phys., 12, 6537–6554, doi:10.5194/acp-12-6537-2012, 2012.

Tzompa-Sosa, Z. A., Mahieu, E., Franco, B., Keller, C. A., Turner, A. J., Helmig, D., Fried, A., Richter, D., Weibring, P., Walega, J., Yacovitch, T. I., Herndon, S. C., Blake, D. R., Hase, F., Hannigan, J. W., Conway, S., Strong, K., Schneider, M., and Fischer, E. V.: Revisiting global fossil fuel and biofuel emissions of ethane, J. Geophys. Res. Atmos., 122, doi:10.1002/2016JD025767, 2017.

Unger, N., Shindell, D. T., Koch, D. M., and Streets, D. G.: Cross influences of ozone and sulfate precursor emissions changes on air quality and climate, Proc. Natl. Acad. Sci., 103, 4377-4380, doi:10.1073/pnas.0508769103, 2006.

van het Bolscher, M., Pereira, J., Spesso, A., Dalsoren, S., van Noije, T., and Szopa, S.: REanalysis of the TROpospheric chemical composition over the past 40 years: A long-term global modeling study of tropospheric chemistry, Max Plank Inst. For Meteorology, Hamburg, Germany, 77, 2008.

Van Dam, B., Helmig, D., Toro, C., Doskey, P., Kramer, L., Murray, K., Ganzeveld, L., and

Seok, B.: Dynamics of ozone and nitrogen oxides at Summit, Greenland: I. Multi-year observations in the snowpack, Atmos. Environ., 123, 268-284, doi:10.1016/j.atmosenv.2015.09.060, 2015.

Walker, T. W., Jones, D. B. A., Parrington, M., Henze, D. K., Murray, L. T., Bottenheim, J. W., Anlauf, K., Worden, J. R., Bowman, K. W., Shim, C., Singh, K., Kopacz, M., Tarasick, D. W., Davies, J., von der Gathen, P., Thompson, A. M., and Carouge, C. C.: Impacts of midlatitude precursor emissions and local photochemistry on ozone abundances in the Arctic, J. Geophys. Res., 117, D01305, doi:10.1029/2011JD016370, 2012.

Wang, Y. H., Jacob, D. J., and Logan, J. A.: Global simulation of tropospheric O_3-NOx-hydro-carbon chemistry 1. Model formulation, J. Geophys. Res.-Atmos., 103, 10713-10725, doi: 10.1029/98JD00158, 1998.

Wang, Y. X., McElroy, M. B., Jacob, D. J., and Yantosca, R. M.: A nested grid formulation for chemical transport over Asia: Applications to CO, J. Geophys. Res., 109, D22307, doi:10.1029/2004JD005237, 2004.

Wesely, M. L.: Parameterization of surface resistances to gaseous dry deposition in regional-scale numerical-models, Atmos. Environ., 23, 1293-1304, doi:10.1016/0004-6981(89)90153-4, 1989.

Wespes, C., Emmons, L., Edwards, D. P., Hannigan, J., Hurtmans, D., Saunois, M., Coheur, P.-F., Clerbaux, C., Coffey, M. T., Batchelor, R. L., Lindenmaier, R., Strong, K., Weinheimer, A. J., Nowak, J. B., Ryerson, T. B., Crounse, J. D., and Wennberg, P. O.: Analysis of ozone and nitric acid in spring and summer Arctic pollution using aircraft, ground-based, satellite

observations and MOZART-4 model: source attribution and partitioning, Atmos. Chem. Phys., 12, 237–259, doi:10.5194/acp- 12-237-2012, 2012.

Wu, S., Mickley, L. J., Jacob, D. J., Logan, J. A., Yantosca, R. M., and Rind, D.: Why are there large differences between models in global budgets of tropospheric ozone?, J. Geophys. Res., 112(D5), D05302, doi:10.1029/02006JD007801, 2007.

Xiao, Y., Logan, J. A., Jacob, D. J., Hudman, R. C., Yantosca, R., and Blake, D. R.: The global budget of ethane and regional constrainsts on U.S. sources, J. Geophys. Res., 113, D21306, doi:10.1029/2007JD009415, 2008.

Yang, J., Honrath, R. E., Peterson, M. C., Dibb, J. E., Sumner, A. L., Shepson, P. B., Frey, M., Jacobi, H.-W., Swanson, A., and Blake, N.: Impacts of snowpack emissions on deduced levels of OH and peroxy radicals at Summit, Greenland, Atmos. Environ., 36, 2523-2534, doi:10.1016/S1352-2310(02)00128-0, 2002.

Yevich, R., and Logan, J. A.: An assesment of biofuel use and burning of agricultural waste in the developing world, Global Biogeochem. Cy., 17, 1095, doi:10.1029/2002GB001952, 2003.

Yu, K., Jacob, D. J., Fisher, J. A., Kim, P. S., Marais, E. A., Miller, C. C., Travis, K. R., Zhu, L., Yantosca, R. M., Sulprizio, M. P., Cohen, R. C., Dibb, J. E., Fried, A., Mikoviny, T., Ryerson, T. B., Wennberg, P. O., and Wisthaler, A.: Sensitivity to grid resolution in the ability of a chemical transport model to simu- late observed oxidant chemistry under high-isoprene conditions, Atmos. Chem. Phys., 16, 4369–4378, doi:10.5194/acp-16-4369- 2016, 2016.

Yue, X., and Unger, N.: Ozone vegetation damage effects on gross primary productivity in the United States, Atmos. Chem. Phys., 14, 9137-9153, doi:10.5194/acp-14-9137-2014, 2014.

Zatko, M. C., Geng, L., Alexander, B., Sofen, E. D., and Klein, K.: The impact of snow nitrate photolysis on boundary layer chemistry and the recycling and redistribution of reactive nitrogen across Antarctica and Greenland in a global chemical transport model, Atmos. Chem. Phys., 16, 2819-2842, doi:10.5194/acpd-16-2819-2016, 2016.

Zhang, H., Wu, S., Huang, Y., and Wang, Y.: Effects of stratospheric ozone recovery on photochemistry and ozone air quality in the troposphere, Atmos. Chem. Phys., 14, 4079-4086, doi:10.5194/acp-14-4079-2014, 2014.

Zhou, X., Beine, H. J., Honrath, R. E., Fuentes, J., Simpson, W., Shepson, P. B., and Bottenheim, J. W.: snowpack photochemical production of HONO: a major source of OH in the Arctic boundary layer in springtime, Geophys. Res. Lett., 28, 21, 4087-4090, 2001.

Atmos. Chem. Phys. Discuss., https://doi.org/10.5194/acp-2017-463
Manuscript under review for journal Atmos. Chem. Phys.
Discussion started: 12 July 2017

Table 1. Surface NO_2 measurements over Europe during 2009/12/01-2010/01/31.

Site ID	Site name	Lat. (°N)	Lon.(°E)	Altitude a.s.l (m)	Technique	Resolution
BE0001R	Offagne	49.88	5.20	430	chemiluminescence	hourly
BE0032R	Eupen	50.63	6	295	chemiluminescence	hourly
DE0001R	Westerland	54.93	8.31	12	NaJ_solution	daily
DK0008R	Anholt	56.72	11.52	40	UV_fluorescence	hourly
FI0096G	Pallas	67.97	24.12	340	chemiluminescence	hourly
GB0014R	High Muffles	54.33	-0.8	267	chemiluminescence	daily
NL0009R	Kollumerwaard	53.33	6.28	1	chemiluminescence	hourly
NO0001R	Birkenes	58.38	8.25	190	glass sinter	daily
NO0039R	Kårvatn	62.78	8.88	210	glass sinter	daily
NO0056R	Hurdal	60.37	11.08	300	glass sinter	daily
SE0005R	Bredkälen	63.85	15.3	404	abs_tube	daily

Atmos. Chem. Phys. Discuss., https://doi.org/10.5194/acp-2017-463
Manuscript under review for journal Atmos. Chem. Phys.
Discussion started: 12 July 2017

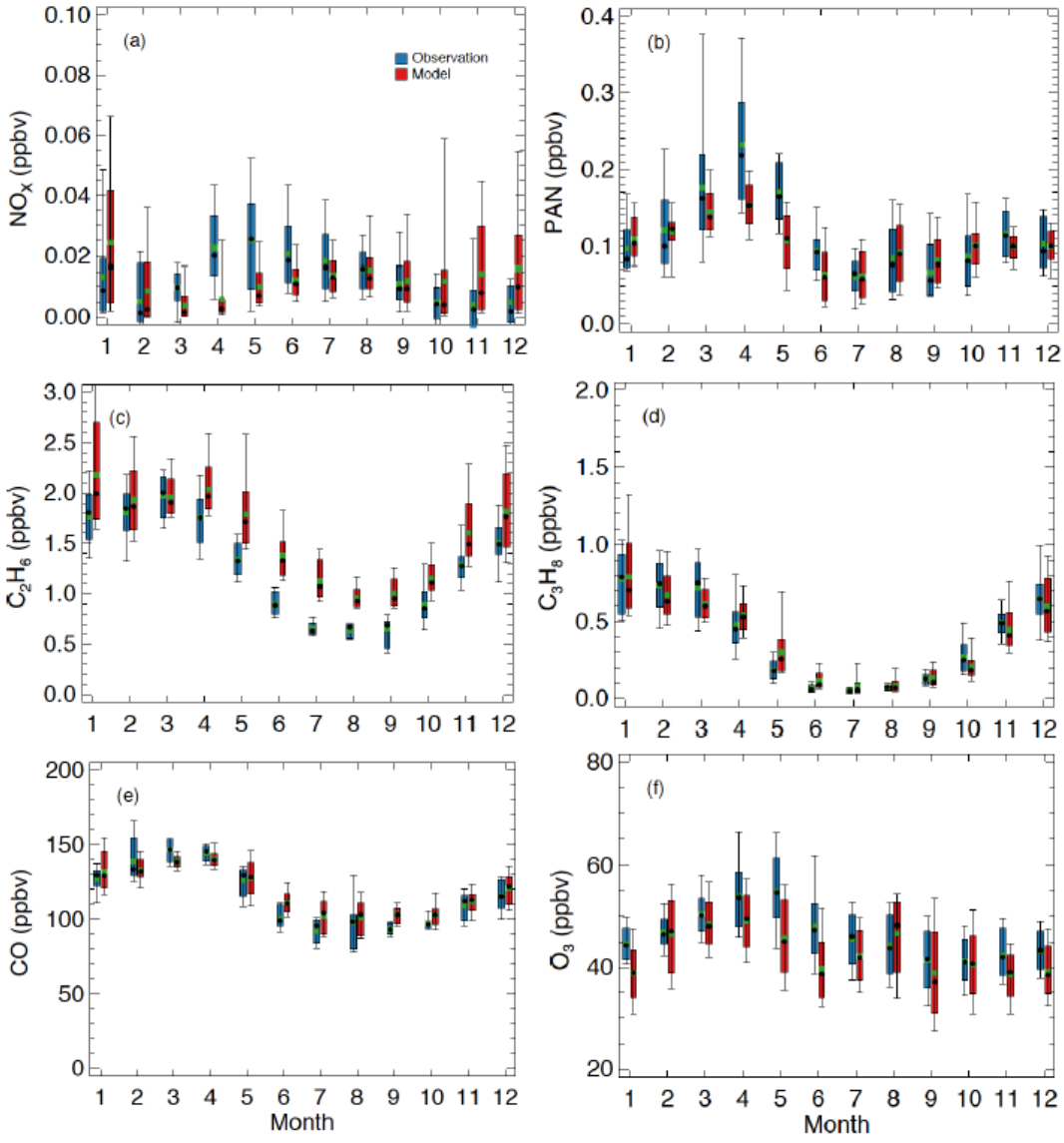

Fig. 1. Box plot comparison for seasonal variations of (a) NO_x, (b) PAN, (c) C_2H_6, (d) C_3H_8, (e) CO, and (f) O_3 between GEOS-Chem model simulations (red) and in-situ measurements (blue) over Summit for the period of 2008/07-2010/06. Data shown are monthly averages during this period. The thick (thin) bars represent the 67% (95%) confidence intervals. Black and green dots represent median and mean values, respectively. The statistics are based on daily averages.

Atmos. Chem. Phys. Discuss., https://doi.org/10.5194/acp-2017-463
Manuscript under review for journal Atmos. Chem. Phys.
Discussion started: 12 July 2017

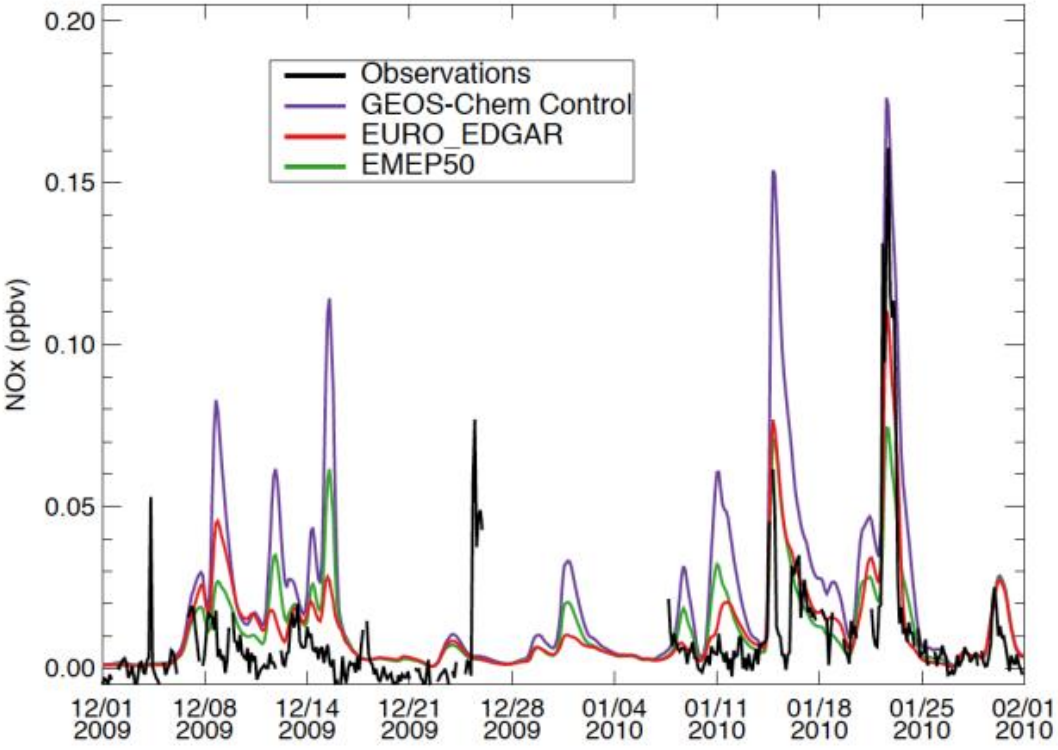

Figure 2. Timeseries of surface NO_x mixing ratios over Summit from observations, GEOS-Chem model control simulations, EURO_EDGAR, and EMEP50 during 2009/12/01-2010/01/31.

Atmos. Chem. Phys. Discuss., https://doi.org/10.5194/acp-2017-463
Manuscript under review for journal Atmos. Chem. Phys.
Discussion started: 12 July 2017

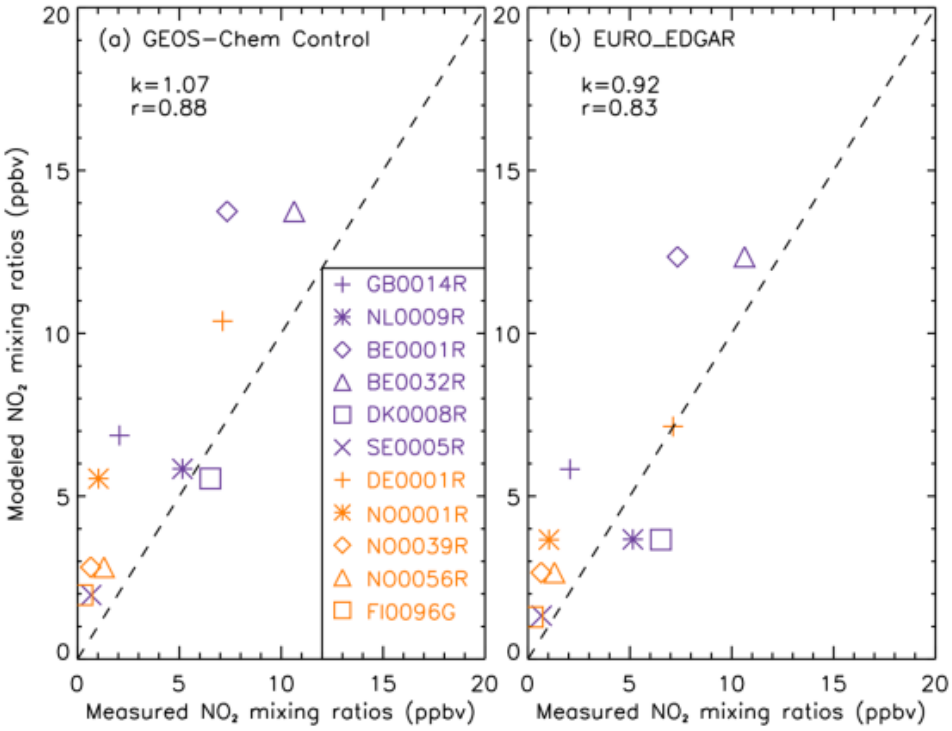

Figure 3. Scatter plots between measured monthly mean NO_2 mixing ratios at 11 observational sites over Europe and model simulations from (a) GEOS-Chem control simulations and (b) EURO_EDGAR during 2009/12/01-2010/01/31; also shown is the corresponding model-to-observation slopes (k) and correlation coefficients (r) for each panel. The dash line is the 1:1 ratio. Explanations of site abbreviations are listed in Table 1.

Atmos. Chem. Phys. Discuss., https://doi.org/10.5194/acp-2017-463
Manuscript under review for journal Atmos. Chem. Phys.
Discussion started: 12 July 2017

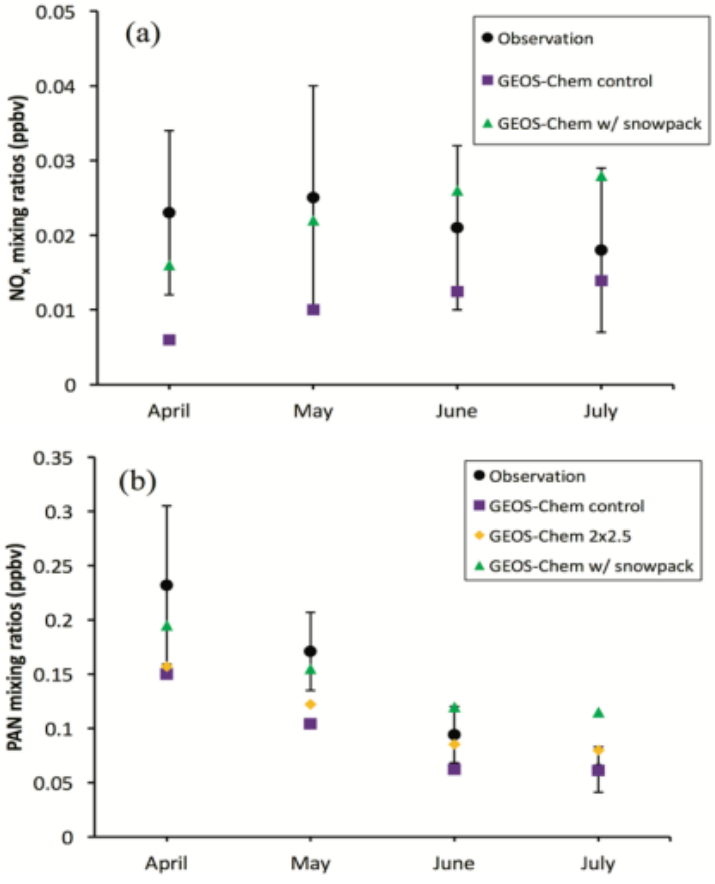

Figure 4. Monthly mean surface (a) NO_x and (b) PAN mixing ratios from observations (black circles), simulations with (green triangles) /without (purple squares) snowpack emissions, and GEOS-Chem simulations with horizontal grid resolution 2° x 2.5° (orange diamonds) over the period of April- July during 07/2008-06/2010. Vertical bars denote standard deviations over the course of observations for each month.

Atmos. Chem. Phys. Discuss., https://doi.org/10.5194/acp-2017-463
Manuscript under review for journal Atmos. Chem. Phys.
Discussion started: 12 July 2017

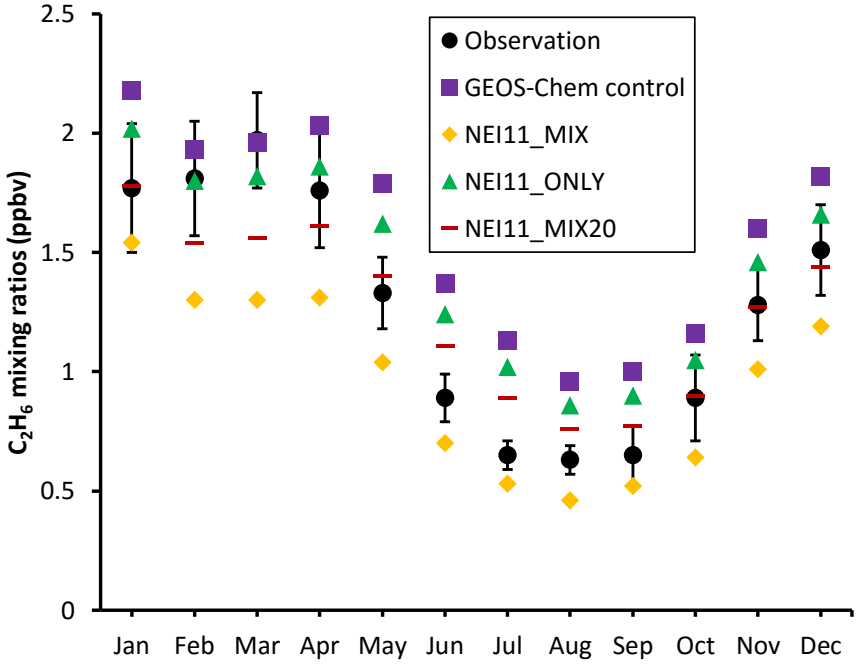

Figure 5. Monthly mean surface C_2H_6 mixing ratios at Summit from observations (black circles), GEOS-Chem model control simulations (purple squares), NEI11_MIX (orange diamond), and NEI11_ONLY (green triangles) simulations during 2008-2010; vertical bars denote the standard deviation over the course of observations for each month.

Atmos. Chem. Phys. Discuss., https://doi.org/10.5194/acp-2017-463
Manuscript under review for journal Atmos. Chem. Phys.
Discussion started: 12 July 2017

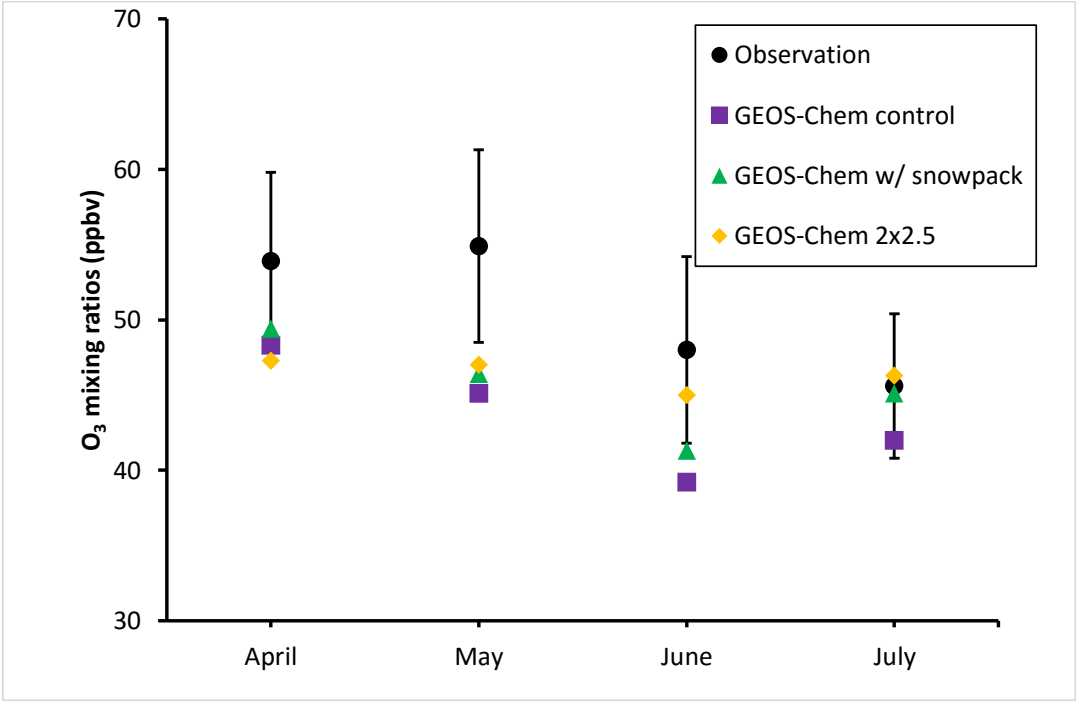

Figure 6. Monthly mean surface O_3 mixing ratios from observations (black circles), GEOS-Chem control runs (purple squares), with snowpack chemistry (green triangles), and horizonal grid resolution 2° x 2.5° (orange diamonds) for April-July. Vertical bars denote the variability over the course of observations for each month.

Atmos. Chem. Phys. Discuss., https://doi.org/10.5194/acp-2017-463
Manuscript under review for journal Atmos. Chem. Phys.
Discussion started: 12 July 2017

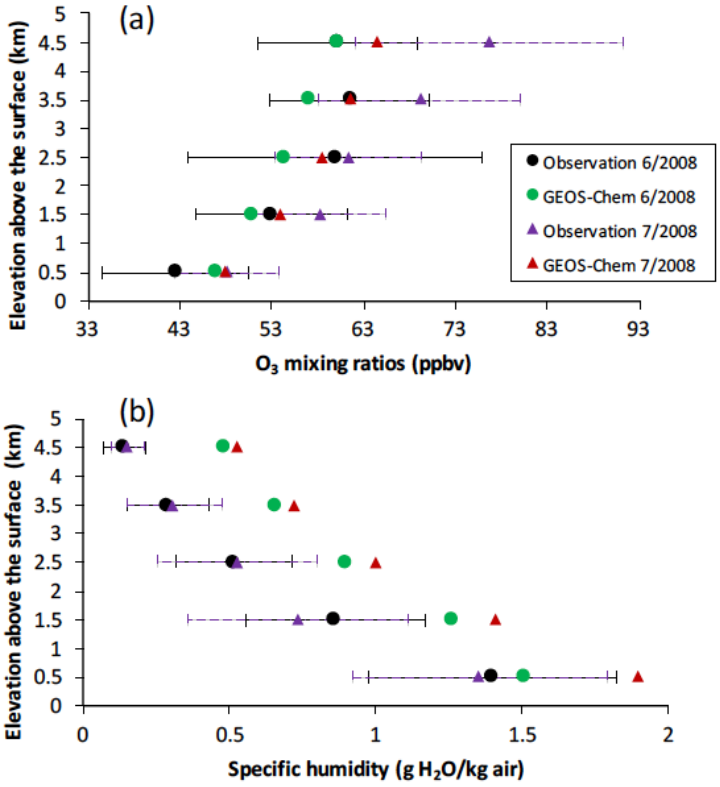

Figure 7. Comparisons of vertical profiles of (a) O_3 and (b) specific humidity between GEOS-Chem simulations and ozonesondes in June and July 2008 respectively, averaged over 1-km altitude bins. Black and green solid circles represent observations and simulations in June 2008 while purple and red triangles denote observations and simulations for July 2008 respectively. Solid and dash horizontal error bars represent observational standard deviations for June and July respectively.